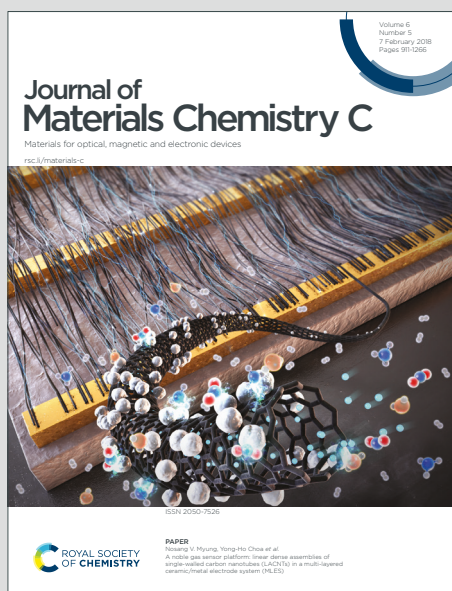


Journal of Materials Chemistry C

Materials for optical, magnetic and electronic devices

Accepted Manuscript

This article can be cited before page numbers have been issued, to do this please use: G. Xia, Q. Shao, K. Liang, Y. Wang, L. Jiang and H. Wang, *J. Mater. Chem. C*, 2020, DOI: 10.1039/D0TC02596H.



This is an Accepted Manuscript, which has been through the Royal Society of Chemistry peer review process and has been accepted for publication.

Accepted Manuscripts are published online shortly after acceptance, before technical editing, formatting and proof reading. Using this free service, authors can make their results available to the community, in citable form, before we publish the edited article. We will replace this Accepted Manuscript with the edited and formatted Advance Article as soon as it is available.

You can find more information about Accepted Manuscripts in the [Information for Authors](#).

Please note that technical editing may introduce minor changes to the text and/or graphics, which may alter content. The journal's standard [Terms & Conditions](#) and the [Ethical guidelines](#) still apply. In no event shall the Royal Society of Chemistry be held responsible for any errors or omissions in this Accepted Manuscript or any consequences arising from the use of any information it contains.

ARTICLE

A Phenyl-removed Strategy for Accessing Efficient Dual-state Emitter at Red/NIR Region: Guided by TDDFT Calculations

Guomin Xia^a, Qingqing Shao^b, Kangli Liang^b, Yigang Wang^b, Lixia Jiang^a, Hongming Wang^{a, b *}

Received 00th January 20xx,
Accepted 00th January 20xx

DOI: 10.1039/x0xx00000x

Developing molecules with efficient dual-state emission at red/NIR region is significant for their broader applications prospect in biological area, but still remains a great challenge. Guided by in-depth TDDFT calculations, herein we firstly demonstrate a phenyl-removed strategy in TPE-merged squaraine dyes for accessing intense red/NIR emission both in solution and crystalline state, on the basis of full decoding the bidirectional TICT/ESIPT mechanism. With removing one phenyl rotator in TPE segment, both less TICT formation and phenyl rotations facilitate the brightest red emission ($\lambda_{em} = 586/622$ nm, $\Phi_{PL} = 57.5\%$) of SQHTPE in solution, while the reserved hydrogen-bonding packing and ESIPT process guarantee the intense red/NIR emission ($\lambda_{em} = 670$ nm, $\Phi_{PL} = 51.2\%$) in its crystalline state. Moreover, efficient red bioimaging in HUVECs has been achieved with naked SQHTPE, which provides a new vision for directly applying squaraine dyes in biological applications.

Introduction

Most of the reported organic luminogens seems to be either emissive in dilute solution but quenched in the aggregation or emissive in the aggregation but quenched in dilute solution, referred to as aggregation-caused quenching (ACQ)^{1,2} or aggregation-induced emission (AIE)³⁻⁶ effect. Yet despite all that, organic materials with well-designed structures can be highly emissive in both solution and solid state, which takes advantage of both ACQ and AIE phenomenon thereby beneficial for broad practical applications.⁷⁻¹⁶ For instance, in 2015 Tang's group accessed propeller-like triphenylamine fluorophores with twisted triphenylethylene (HTPE, generally regarded as AIE building block^{17,18}) showing intense blue to cyan emission in both solution and solid states.¹⁹ Very recently, Zhu and co-workers developed planar diphenyl-diacetylene structures with distorted cyanostilbenes and long alkyl side chains featuring bright blue to green emission in solution, amorphous and crystalline state.²⁰ In those molecules, the delicate balance between intramolecular rigidity and twisted conformations is regarded as the crucial factor for accessing their highly efficient dual-state emission (DSE), since the former is mentioned to restrict free intramolecular motions in solution, while the latter is to resist intermolecular π - π stacking in solid state. Upon this guidance, it is very reasonable to speculate that those luminogens

exhibit a short-wavelength emission in dual state due to their decreased molecular conjugations and highly prevented exciton interactions in twisted configurations. As such, a novel strategy for accessing dual-state efficient luminogens at the red/NIR region remains a huge challenge but highly desired, especially in biologic area.^{21,22}

Squaraine dyes (SQs) have attracted much attention in advanced fields due to its excellent photoelectrical properties, but are still greatly limited by its typical ACQ behaviours.²³⁻²⁸ Recently we have been devoted to the exploration of novel SQs with solid-state emission and understanding of the relationship among their molecular structures, self-assembled morphologies and photophysical properties.²⁹⁻³¹ From our latest study on SQs with DSE behaviour,³² two interlaced effects aroused us a great deal of confusion due to the insertion of tetraphenylethylene (TPE) group into SQs: 1) on the one hand the internal phenyl rotations in TPE segment was regarded to facilitate the non-radiative decays, 2) while on the other hand the suppressed twisted intramolecular charge transfer (TICT)³³⁻³⁷ process on account of the big entire TPE segment was regarded to facilitate radiative decays. These two opposing results thus resulted in an ambiguous mechanism of its laboratorial low emission efficiency (Φ_{PL}) in dilute solution, in spite of its desired high Φ_{PL} through an excited-state intramolecular proton transfer (ESIPT)³⁸⁻⁴¹ channel in crystalline state. As such, it is of great necessity and urgency to further understand the two factors affecting emission in this system. Guided by TDDFT calculations, we reported here a phenyl-removed strategy in TPE-merged squaraine dyes for accessing intense red/NIR emission in dual state. All the results would be benefit for the design and controlling of efficient DSE-active molecules in the near future.

^a Institute for Advanced Study and College of Chemistry, Nanchang University, 999, Xuefu Road, Nanchang, 330031, P.R. China.

^b School of Materials Science and technology, Nanchang University, 999, Xuefu Road, Nanchang, 330031, P.R. China

* hongmingwang@ncu.edu.cn

Electronic Supplementary Information (ESI) available: synthesis, characterization, calculations and crystal data. See DOI:10.1039/x0xx00000x

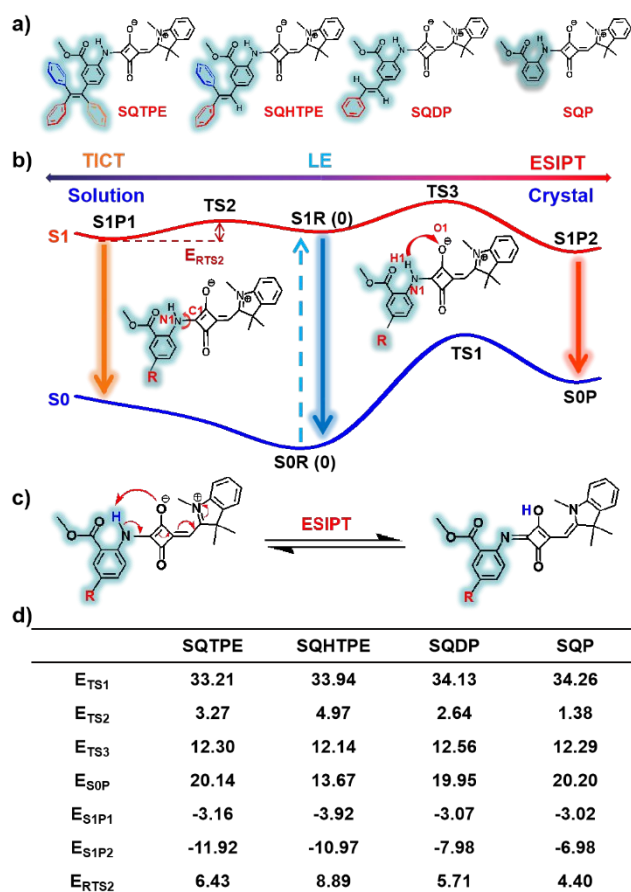


Fig. 1 a) Structures of SQTPE, SQHTPE, SQDP and SQP; b) Schematic illustrations of the bidirectional TICT/ESIPT mechanism in different state; c) Reaction equation of ESIPT process in these SQs through proton H transfers from N to O atom of central ring; d) Computed relative energy of important stationary points on reaction potential energy surface of SQTPE, SQHTPE, SQDP and SQP (unit: kcal mol⁻¹).

Results and discussion

Molecular design, TDDFT calculations and synthesis

To gain deep insights into this systems, we thus designed SQTPE, SQHTPE, SQDP and SQP with gradually removed phenyl rotator in the extended ethylene in TPE segment (Fig. 1a), and next detailedly computed their photophysical and photochemical mechanisms (Supporting Information).⁴²⁻⁴⁴ The calculated corresponding ground and excited potential energy surface of four molecules in toluene as a function of C1-N1 rotations in TICT formation and ESIPT processes were showed in Fig. 1b, Fig. S1-3 and Table S1. From the calculations, it was easy to conclude that the dual emission of all SQs analogues can be responded by their favourable local excited (LE)/TICT process with the distortion of C1-N1 bond in S1 state occurred in solution, while their red-shifted single emission followed the ESIPT process from N1 to O1 atoms in crystalline state due to TICT formation was strictly prohibited. It is interesting to note that the energy barriers of TICT formations (E_{TS2}) in those analogues was in the order of SQHTPE > SQTPE > SQDP >> SQP, strongly suggesting that the LE state should populate most largely in SQHTPE than that in other SQ molecules, thereby facilitating its strongest emission in LE state. Once reached TICT state, the reversion of C1-N1 bond distortion for SQHTPE was also the most difficult to take place because of the highest

reversion energy barrier (E_{RTS2}), which indicated a quickly thermodynamic equilibrium with the minimum vibrations thus making SQHTPE possessed the strongest emission in TICT states as well. In contrast, both low energy barrier (E_{TS2}) and relative energy (E_{S1P1}) would cause easily an inverse TICT process of much-anticipated SQTPE, which would greatly increase vibrational relaxation thus resulting its low emission in solution, even if taking no account of the internal phenyl rotations in its TPE segment. In other words, it seems that the solution Φ_{PL} of SQHTPE would be much better than that of SQTPE, together with its twisted HTPE segment for suppressing π - π stacking and similar energy barriers of TS3 in ESIPT channel (Fig. 1c, d), permitting SQHTPE a potential highly efficient DSE-active molecule. Besides, the difference between the emission band maxima in solution and solid state (define as DSE shift) would be expected to become large from the TDDFT calculations (Fig.S1).

These theoretical calculations encouraged us to experimentally verify the phenyl-removed strategy in brightening the emission and further helped us to thoroughly evaluate the interlaced effects mentioned above. Therefore, those target four analogues were elaborately synthesized, and the overall synthetic routes of reaction intermediates and desired derivatives were shown in detail in Scheme S1-5, with fully characterized by ¹H NMR, ¹³C NMR and mass spectroscopy (details in Supporting Information). After that, their various emission behaviours and corresponding mechanisms in solution and solid state were then discussed in detail.

The photophysical properties of SQs in solution

To examine whether the phenyl-removed strategy can brighten solution emission for the designed molecules, the photophysical properties of all compounds were firstly investigated in common solvents with different polarity (Fig. S4 and Table S2). It could be found that a rather good mirror image relation between their dual absorption and emission spectra in various solvents, which can be associated with their LE and TICT states with Stokes shift around 15 and 80 nm, respectively. Notably, the emission of SQTPE was red-shifted with the Φ_{PL} clearly decreased upon increasing the solvent polarity from hexane (22.3%), CH₂Cl₂ (11.8%) to DMSO (10.2%), furtherly proved its LE/TICT electronic characters.⁴⁵ While in toluene, SQTPE exhibited a brightest red emission efficiency ($\Phi_{PL} = 26.9\%$) at 579 nm together with a shoulder peak at 616 nm (Table 1), which may resulted from excellent solvation effect between aromatic SQTPE and toluene.¹⁹ As for protic CH₃OH, it was able to interact with SQTPE via multiple hydrogen-bonding interactions, which may lead to a net stabilization of its ground state and nonradiation of its excited state for an abnormal blue-shift in the spectra and the lowest Φ_{PL} .⁴⁶ Very similar spectral phenomena were also observed in SQHTPE, SQDP and SQP, suggesting their very analogical ground/excited-state electronic structures in solution. Besides, all the fluorescence decay profiles of those luminogens in solution were well fitted by using a single exponential function with two fluorescence lifetimes in the nanosecond time scale (Table S2, and Fig. S5).

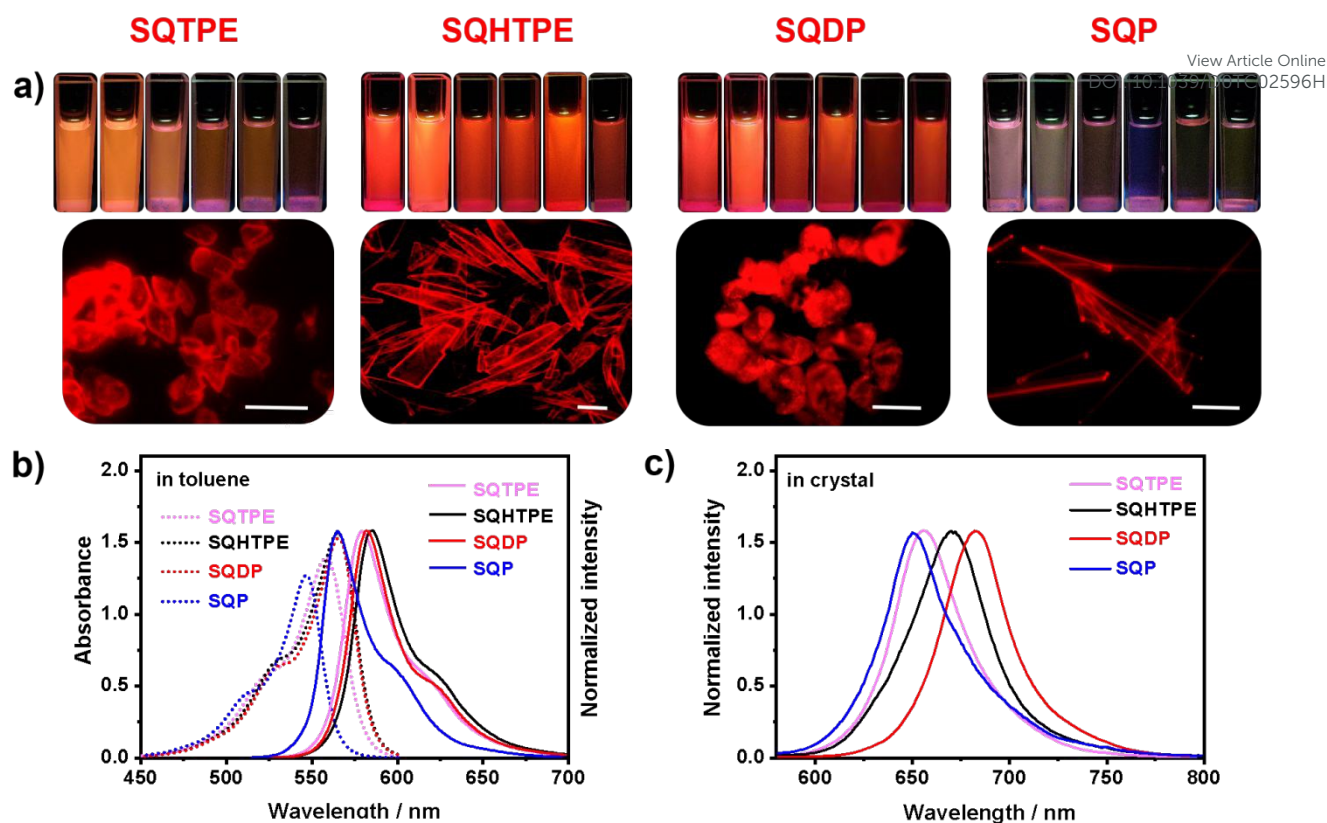


Fig. 2 a) Emissive photographs of SQTPE, SQHTPE, SQDP and SQP in solution (10 μM, from left to right: Toluene, Hexane, THF, CH₂Cl₂, DMSO and CH₃OH) and in crystalline state (under 365 nm UV illumination, scale bar: 50 μm); b) absorption/emission spectra of the luminogens in toluene; and c) in the crystalline state ($\lambda_{\text{ex}} = 500$ nm).

As shown in Fig. 2b, SQHTPE exhibited obvious red-shifted but stronger absorption profiles with maximum peak (λ_{ab}) at 537/568 nm in toluene, and these changes were also recorded in their emissions with (maximum peak) λ_{em} at 586/622 nm, suggesting its bit larger conjugation than SQTPE in solution. The emission intensity of SQHTPE, as expected, underwent a great enhancement with Φ_{PL} increased up to 57.5% in toluene (Table 1), directly verifying our theoretical prediction. As for SQDP, it exhibited a very similar absorption (536/568 nm) and emission spectra (582/621 nm) in toluene, suggesting a comparative length conjugation as compared to that in SQHTPE (Fig. 2b). The Φ_{PL} of SQDP, notably, was also enhanced to 42.7%, although its TICT formation hold a decreased energy barrier (2.64 kcal mol⁻¹) as compared to that in SQTPE (3.27 kcal mol⁻¹). From all the theoretical and experimental data, we can perhaps draw two main conclusions: 1) both less TICT formation and phenyl rotations simultaneously facilitated the radiative decays thus resulting in the brightest red emission ($\Phi_{\text{PL}} = 57.5\%$) of SQHTPE in toluene, when removing one phenyl rotator in TPE segment of SQTPE; and 2) by continuous remove of another phenyl rotator, the obtained SQDP still exhibited a brighter red emission ($\Phi_{\text{PL}} = 42.7\%$) in toluene, suggesting the further reduced phenyl rotations exerted greater effect on its emission behaviour than its relatively more TICT formation. While in SQP, the obvious blue-shifted behaviours both in absorption ($\lambda_{\text{ab}} = 508/544$ nm) and

emission ($\lambda_{\text{em}} = 558/593$ nm) in toluene meant that it was in obviously less conjugation than the others (Fig. 2b, Table 1), and preferable TICT formation with lowest barrier energy (1.38 kcal mol⁻¹) accompanying with lowest reversion energy barrier (4.40 kcal mol⁻¹) gave good explanation to its clearly lowest Φ_{PL} of 11.3% in toluene (Table 1). All the measured spectral data are well consistent with that of theoretical calculation.

Structural analysis and solid-state emission of SQs

For the proton transfer channel, it showed that the energy

Table 1. Summary of optical properties of the luminogens (λ : nm, Φ_{PL} : %^a).

Sample	in toluene (10 μM)				in crystal			
	λ_{ab}	λ_{em}	Φ_{PL}	Sf ^b	λ_{em}	Φ_{PL}	Sf ^c	Df ^d
SQTPE	532/560	579/616	26.9	19	656	73.1	96	77
SQHTPE	537/568	586/622	57.5	18	670	51.2	102	84
SQDP	536/568	582/621	42.7	14	682	40.5	114	100
SQP	508/544	558/593	11.3	14	675	8.1	131	117

^a Absolute Φ_{PL} were determined using a Horiba FL-3018 Integrating Sphere;

^b The Stokes shift of LE state;

^c The Stokes shift of ESIPST state;

^d DSE shift: $Df = \lambda_{\text{em}}^{\text{crystal}} - \lambda_{\text{LE}}^{\text{toluene}}$.

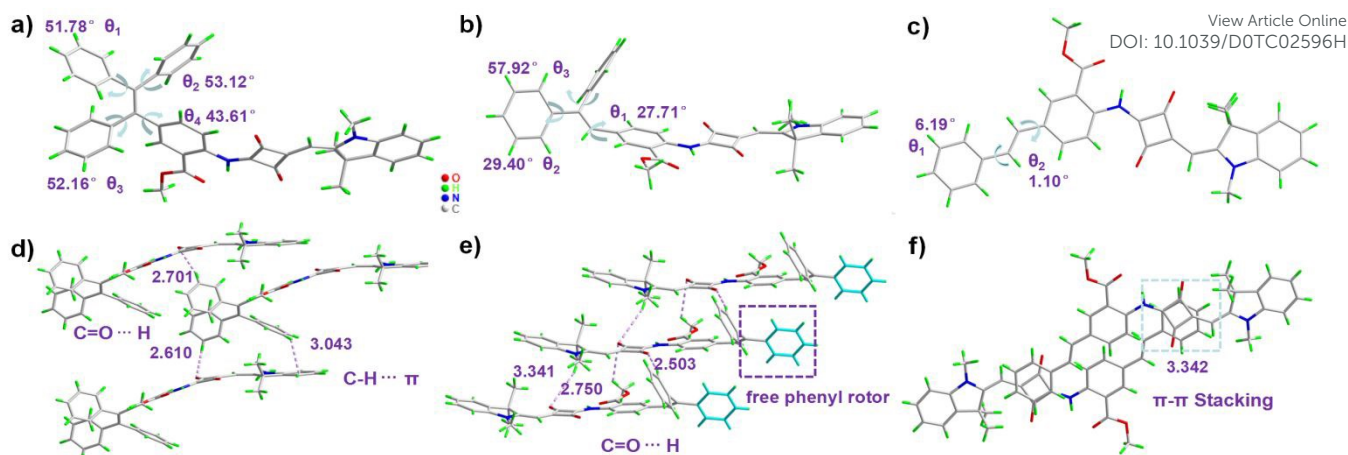


Fig. 3 The dihedral angles between vinyl bond and phenyl rotors in a) SQTPPE, b) SQHTPE, c) SQDP crystals. Intermolecular interactions including no π - π interactions with d) no free phenyl rotors in SQTPPE crystals, e) one free phenyl rotor in SQHTPE and f) weak π - π interactions in SQDP.

barriers of TS3 were almost equaled for these four molecules (Fig. 1d), which indicated that there was little effect on their ESIPT process via remove of substituted phenyl rotator. In fact, ESIPT process may mainly determine their single long wavelength emission up to red/NIR region (Table 1), and their intermolecular packing modes would greatly dominate their emission efficiency in crystalline state for those four analogues. As such, to deeply understand their structure-property relationships, single crystals of SQTPPE, SQHTPE and SQDP were then obtained for X-ray crystallography in CH_2Cl_2 /Hexane mixtures (Table S3 and Fig. S6-8), so did their corresponding well-ordered crystalline assemblies (Fig. S9-12, preparation methods and characterizations in detail see Supporting Information). As for the identical SQP segments in these derivatives, two types of strong intramolecular $\text{C}=\text{O}\cdots\text{H}$ hydrogen bonding interactions would greatly facilitate their intramolecular planarity and rigidity in solution, and two methyl fork chains in the indoline moiety were very helpful for preventing partial π - π stacking. Additionally, the triple carbonyl groups in central four-membered ring and methyl ester were particularly in favour of forming multiple intermolecular hydrogen bonding interactions for potentially generating hydrogen-bonding crystals. Thus, these inherent structural characteristics were rewarding for the building of these luminogens with potential DSE behaviour. Detailed single crystals analyses of these three analogous have been deciphered in the Supporting Information (Fig. S6-8).

In SQTPPE and SQHTPE crystals, similar twisting TPE and HTPE segments (Fig. 3a-b) helped to fully suppressed intermolecular π - π interactions in the construction of crystalline assemblies (Fig. 3d-e), and the free phenyl rotors detected in SQHTPE crystals can be responded to its relatively lower Φ_{PL} of 51.2% at 670 nm than that of 73.1% at 656 nm in SQTPPE crystals without any free phenyl rotors (Fig. 3d-e). For SQDP crystals, the dihedral angle between the phenyl group and vinyl determined to be only 1.10° and 6.19° (Fig. 3c), implying extended conjugated SQDP exhibited an exceedingly planarized conformation in crystals on the whole. In spite of multiple intermolecular hydrogen bonding interactions in the

SQDP crystals, there also exhibited weak intermolecular π - π interactions in 3.342 Å between central four-member ring and distal phenyl group in adjacent SQDP molecule (Fig. 2f). This mode permitted its crystalline assemblies showed an obviously red-shifted λ_{em} centered at 682 nm with low Φ_{PL} of 40.5%, in comparison with λ_{em} of 656 nm in SQTPPE crystals (Table 1). As for the low Φ_{PL} of 8.1% in SQP crystals, this might be ascribed to their limited conjugation and favourable intermolecular π - π interactions in condensed phase. From Table 1, it was found that the DSE shifts of SQTPPE, SQHTPE, SQDP and SQP were 77, 84, 100 and 117 nm, respectively, due to their emissive mechanisms all changed from LE/TICT in solution to ESIPT in crystalline state. To the best of our knowledge, which represents the largest DSE shift among all the DSE molecules (Table S5).

Besides, these four amorphous assemblies, obtained by grinding of their crystalline sample and confirmed by Powder X-ray diffraction (PXRD, Fig. S10), exhibited rapidly decreased intensity of their emission (Fig. S12), which can be mainly ascribed to that their amorphous aggregates were in loosely stacked state that cannot well restrict the intramolecular rotations. These emission quenching behaviours from crystalline-amorphous transformation were also responsible for their observed ACQ from the tests in THF/water mixtures (Fig. S13), suggesting a typical crystalline-induced emission (CIE) effect.⁴⁷⁻⁵⁰ Similarly, their fluorescence decay profiles in amorphous or crystalline state were also well fitted by using a single exponential function with one fluorescence lifetimes in the nanosecond time scale (Fig. S12, and Table S4).

Cell bioimaging

As we all known, typical SQ derivatives normally need cumbersome encapsulation to avoid nonfluorescent aggregation and biological nucleophiles attacking in cell bioimaging.⁵¹⁻⁵⁵ Here we established a really simple live-cell imaging strategy by using "naked" SQHTPE regardless of those two disadvantages. As shown in Fig. S14, SQHTPE was quite stable in the presence of common biological results indicated a very satisfactory biocompatibility of SQHTPE to the

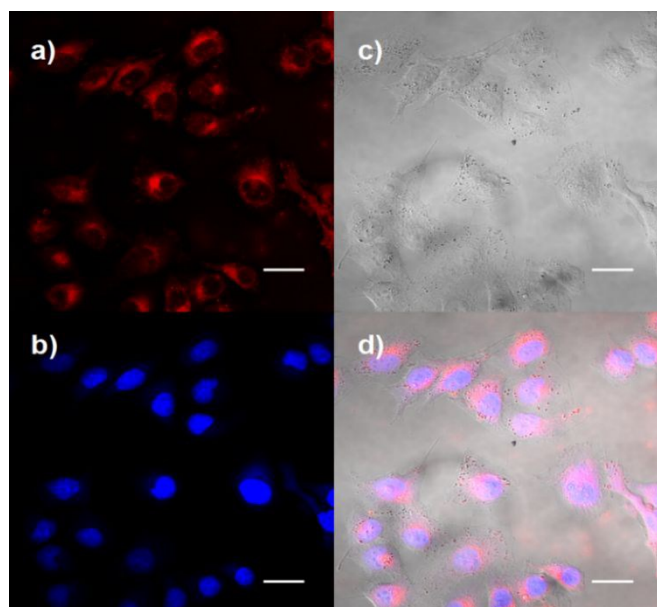


Fig. 4. Confocal fluorescence images of HUVECs; Incubated with a) $10 \mu\text{g mL}^{-1}$ of SQHTPE ($\lambda_{\text{ex}} = 514 \text{ nm}$) followed by b) DAPI for another 30 min ($\lambda_{\text{ex}} = 405 \text{ nm}$); c) Bright field and d) Merged imaging of a + b; Scale bar: $50 \mu\text{m}$.

nucleophiles and lab light. Furtherly, *in vitro* cell viability HUVECs thereby favourable for cell imaging (Fig. S15). As such, a low concentration of $10 \mu\text{g mL}^{-1}$ SQHTPE in culture medium solution was used for fluorescence cell imaging with HUVECs. After incubated with SQHTPE for 30 min, the HUVECs exhibited bright red fluorescence from areas surrounding the DAPI-stained nuclei (Fig. 4). For this, phagocytosis might be the possible mechanism for intracellular uptake of SQHTPE, which exhibited red emission in HUVECs no matter in monomeric or aggregated states. All the results demonstrated that SQHTPE could efficiently image cells without any encapsulation.

Conclusions

In summary, we demonstrated the first time of a phenyl-removed strategy in TPE-merged SQs for accessing efficient emission both in solution and crystalline state, on the basis of fully deciphering the bidirectional TICT/ESIPT mechanism in these analogues by in-depth TDDFT. With removing one phenyl rotator in TPE segment, both less TICT formation and phenyl rotations allowed the brightest red emission ($\Phi_{\text{PL}} = 57.5\%$ at $586/622 \text{ nm}$) of SQHTPE in solution. Meanwhile, the reserved hydrogen-bonding packing mode and ESIPT process in SQHTPE crystals responded to its intense red/NIR emission ($\Phi_{\text{PL}} = 51.2\%$ at 670 nm). Efficient red bioimaging in HUVECs has been achieved with naked SQHTPE, promising these molecules potential in biological applications. We believe this phenyl-removed strategy could be not only very helpful for comprehensively considering the impact factors in DSE-active molecules, but also practical for flourishing their constructions in view of that there are many AIE-active luminogens with TPE merged.

Conflicts of interest

There are no conflicts to declare.

View Article Online
DOI: 10.1039/D0TC02596H

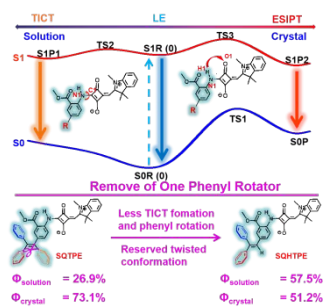
Acknowledgements

We are grateful to the support of the National Natural Science Foundation of China (21363014 and 21103082). This work was also supported by the Natural Science Foundation of the Jiangxi Province of China (Grant No. 20142BCB23003 and 20143ACB21021).

Notes and references

1. T. Förster, K. Kasper, *Z. Phys. Chem.* 1954, **1**, 275-277.
2. J. B. Birks, *J. Lumin.* 1970, **4**, 69.
3. Y. Hong, J. W. Y. Lam, B. Z. Tang, *Chem. Commun.* 2009, **29**, 4332.
4. J. Mei, N. L. C. Leung, R. T. K. Kwok, J. W. Y. Lam, B. Z. Tang, *Chem. Rev.* 2015, **115**, 11718.
5. Y. Hong, J. W. Y. Lam, B. Z. Tang, *Chem. Soc. Rev.* 2011, **40**, 5361.
6. J. Mei, Y. Hong, J. W. Y. Lam, A. Qin, Y. Tang, B. Z. Tang, *Adv. Mater.* 2014, **26**, 5429.
7. Y. Lei, Q. Liu, L. Dong, Z. Cai, J. Shi, J. Zhi, B. Tong, Y. Dong, *Chem. Eur. J.* 2018, **24**, 1.
8. J. Wang, Z. Liu, S. Yang, Y. Lin, Z. Lin, Q. Ling, *Chem. Eur. J.* 2018, **24**, 322.
9. P. Gopikrishna, P. K. Iyer, *J. Phys. Chem. C* 2016, **120**, 26556.
10. M. Li, Y. Nu, X. Zhu, Q. Peng, H. Lu, A. Xia, C. F. Chen, *Chem. Commun.* 2014, **50**, 2993.
11. Y. Sun, T. Wu, F. Zhang, R. Zhang, M. Wu, Y. Wu, X. Liang, K. Guo, Jie Li, *Dyes and Pigments* 2018, **149**, 73.
12. M. Huang, R. Yu, K. Xu, S. Ye, S. Kuang, X. Zhu, Y. Wan, *Chem. Sci.* 2016, **7**, 4485.
13. Y. Xu, L. Ren, D. Dang, Y. Zhi, X. Wang, L. Meng, *Chem. Eur. J.* 2018, **24**, 10383.
14. D. K. Singh, K. Jang, J. Kim, J. Lee, I. Kim, *ACS Comb. Sci.* 2019, **21**, 408.
15. Y. Lei, W. Dai, Z. Liu, S. Guo, Z. Cai, J. Shi, X. Zheng, J. Zhi, B. Tong, Y. Dong, *Mater. Chem. Front* 2019, **3**, 284.
16. C. H. Zhao, A. Wakamiya, Y. Inukai, S. Yamaguchi, *J. Am. Chem. Soc.* 2006, **128**, 15934.
17. X. Zhang, Z. Chi, H. Li, B. Xu, X. Li, S. Liu, Y. Zhang, J. Xu, *J. Mater. Chem.* 2011, **21**, 1788.
18. Z. Yang, Z. Chi, T. Yu, X. Zhang, M. Chen, B. Xu, S. Liu, Y. Zhang, J. Xu, *J. Mater. Chem.* 2009, **19**, 5541.
19. G. Chen, W. Li, T. Zhou, Q. Peng, D. Zhai, H. Li, W. Z. Yuan, Y. Zhang, B. Z. Tang, *Adv. Mater.* 2015, **27**, 4496.
20. H. Wu, Z. Chen, Chi, W.; B. Kaur, L. Gu, C. Qian, B. Wu, B. Yue, G. Liu, G. Yang, L. Zhu, Y. Zhao i, *Angew. Chem. Int. Ed.* 2019, **58**, 11419.
21. J. Mei, Y. Huang, H. Tian, *Appl. Mater. Interfaces* 2018, **10**, 12217.
22. A. Shao, Y. Xie, S. Zhu, Z. Guo, S. Zhu, J. Guo, P. Shi, T. D. James, H. Tian, W. H. Zhu, *Angew. Chem. Int. Ed.* 2015, **54**, 7275.

23. S. Sreejith, P. Carol, P. Chithra, A. Ajayaghosh, *J. Mater. Chem.* 2008, **18**, 264.
24. J. J. McEwen, K. J. Wallace, *Chem. Commun.* 2009, **42**, 6339.
25. G. Xia, H. Wang, *J. Photochem. and Photobiol. C: Photochem. Rev.* 2017, **31**, 84.
26. J. Li, B. Lv, D. Yan, S. Yan, M. Wei, M. Yin, *Adv. Funct. Mater.* 2015, **25**, 7442.
27. S. Yang, J. You, J. Lan, G. Gao, *J. Am. Chem. Soc.* 2012, **134**, 11868.
28. C. Ji, Q. Gao, X. Dong, W. Yin, Z. Gu, Z. Gan, Y. Zhang, M. Yin, *Angew. Chem. Int. Ed.* 2018, **57**, 11384.
29. G. Xia, Z. Jiang, S. Shen, K. Liang, Q. Shao, Z. Cong, H. Wang, *Adv. Opt. Mater.* 2019, **7**, 1801549.
30. G. Xia, S. Shen, X. M. Hu, Z. Jiang, K. Xu, H. Wang, *Chem. Eur. J.* 2018, **24**, 13205.
31. K. Liang, Q. Shao, G. Xia, Y. Wang, L. Jiang, L. Hong, H. Wang, *Dyes and Pigments* 2020, **173**, 107926.
32. Q. Shao, K. Liang, H. Ling, Y. Wang, Z. Yan, G. Xia, H. Wang, *J. Mater. Chem. C* 2020, **8**, 4549.
33. W. Retting, *Angew. Chem. Int. Ed.* 1986, **25**, 971.
34. H. Naito, K. Nishino, Y. Morisaki, K. Tanaka, Y. Chujo, *Angew. Chem. Int. Ed.* 2017, **56**, 254.
35. S. Sasaki, G. P. C. Drummen, G. i. Konishi, *J. Mater. Chem. C* 2016, **4**, 2731.
36. K. Li, Y. Liu, Y. Li, Q. Feng, H. Hou, B. Z. Tang, *Chem. Sci.* 2017, **8**, 7258.
37. Y. Zhang, J. Zhang, J. Shen, J. Sun, K. Wang, Z. Xie, H. Gao, B. Zou, *Adv. Opt. Mater.* 2018, **6**, 1800956.
38. V. S. Padalkar, S. Seki, *Chem. Soc. Rev.* 2016, **45**, 169.
39. J. Zhao, S. Ji, Y. Chen, H. Guo, P. Yang, *Phys. Chem. Chem. Phys.* 2012, **14**, 8803.
40. J. E. Kwon, S. Y. Park, *Adv. Mater.* 2011, **23**, 3615.
41. K. C. Tang, M. J. Chang, T. Y. Lin, H. A. Pan, T. C. Fang, K. Y. Chen, W. Y. Hung, Y. H. Hsu, P. T. Chou, *J. Am. Chem. Soc.* 2011, **133**, 17738.
42. M. J. Frisch, G. W. Trucks, H. B. Schlegel, G. E. Scuseria, M. A. Robb, J. R. Cheeseman, G. Scalmani, V. Barone, B. Mennucci, G. A. Petersson, H. Nakatsuji, M. Caricato, X. Li, H. P. Hratchian, A. F. Izmaylov, J. Bloino, G. Zheng, J. L. Sonnenberg, M. Hada, M. Ehara, K. Toyota, R. Fukuda, J. Hasegawa, M. Ishida, T. Nakajima, Y. Honda, O. Kitao, H. Nakai, T. Vreven, J. A. Jr. Montgomery, J. E. Peralta, F. Ogliaro, M. Bearpark, J. J. Heyd, E. Brothers, K. N. Kudin, V. N. Staroverov, R. Kobayashi, J. Normand, K. Raghavachari, A. Rendell, J. C. Burant, S. S. Iyengar, J. Tomasi, M. Cossi, N. Rega, J. M. Millam, M. Klene, J. E. Knox, J. B. Cross, V. Bakken, C. Adamo, J. Jaramillo, R. Gomperts, R. E. Stratmann, O. Yazyev, A. J. Austin, R. Cammi, C. Pomelli, J. W. Ochterski, R. L. Martin, K. Morokuma, V. G. Zakrzewski, G. A. Voth, P. Salvador, J. J. Dannenberg, S. Dapprich, A. D. Daniels, O. Farkas, J. B. Foresman, J. V. Ortiz, J. Cioslowski, and D. J. Fox, Gaussian, Inc., Wallingford CT, 2009.
43. C. T. Lee, W. T. Yang, R. G. Parr, *Phys. Rev. B* 1988, **37**, 785.
44. A. D. Becke, *J. Chem. Phys.* 1993, **98**, 5648.
45. Z. Guo, Z. Jin, J. Wang, J. Pei, *Chem. Commun.* 2014, **50**, 6088. DOI: 10.1039/D0TC02596H
46. P. Xu, T. Gao, M. Liu, H. Zhang; W. Zeng, *Analyst* 2015, **140**, 1814.
47. H. Naito, Y. Morisaki, Y. Chujo, *Angew. Chem. Int. Ed.* 2015, **54**, 5084.
48. Y. Dong, J. W. Y. Lam, A. Qin, Z. Li, J. Sun, H. H.-Y. Sung, I. D. Williams, B. Z. Tang, *Chem. Commun.* 2007, **1**, 40.
49. P. Galer, R. C. Korošec, M. Vidmar, B. Šket, *J. Am. Chem. Soc.* 2014, **136**, 7383.
50. Y. Lin, G. Chen, L. Zhao, W. Z. Yuan, Y. Zhang, B. Z. Tang, *J. Mater. Chem. C* 2015, **3**, 112.
51. E. Arunkumar, C. C. Forbes, B. C. Noll, B. D. Smith, *J. Am. Chem. Soc.* 2005, **127**, 3288.
52. J. R. Johnson, N. Fu, E. Arunkumar, W. M. Leevy, S. T. Gammon, D. Piwnica-Worms, B. D. Smith, *Angew. Chem. Int. Ed.* 2007, **46**, 5528.
53. S. Sreejith, J. Joseph, M. Lin, N. V. Menon, P. Borah, H. J. Ng, Y. X. Loong, Y. Kang, S. W.-K. Yu, Y. Zhao, *ACS Nano* 2015, **9**, 5695.
54. T. Liu, X. Liu, Y. Zhang, M. V. Bondar, Y. Fang, K. D. Belfield, *Eur. J. Org. Chem.* 2018, **30**, 4095.
55. R. Yi, P. Das, F. Lin, B. Shen, Z. Yang, Y. Zhao, L. He, Y. Hong, R. Hu, Jun. Song, J. Qu, L. Liu, *Opt. Express* 2019, **27**, 12360.



We report here a phenyl-removed strategy in TPE-merged squaraine dyes for accessing intense red/NIR emission both in solution and crystalline state, guided by in-depth TDDFT calculations.